Androgen rapidly activates phosphorylation signaling pathways in Sertoli cells

RUI SUN*, YE DU*, LIAN GAO*, ZHU WANG, HUI LIANG, YING ZHANG and QIONG DENG

Department of Urology, Affiliated Longhua Hospital, Southern University of Science and Technology, Shenzhen, Guangdong 518109, P.R. China

Received December 16, 2025; Accepted May 28, 2026

DOI: 10.3892/etm.2026.13224

Abstract. Androgen-activated phosphorylation signaling pathways are of critical importance during spermatogenesis. The present study comprehensively analyzed androgen-activated phosphorylation signaling pathways in testicular Sertoli cells. Primary cultured mouse Sertoli cells were treated with testosterone for varying durations. Using tandem mass tag-labeled phosphoproteomics technology combined with Mfuzz clustering and functional enrichment analysis, key phosphorylation signaling pathways were identified. Mass spectrometry revealed 13,015 quantifiable phosphorylation sites, and Mfuzz clustering of expression pattern categorized 330 proteins into 6 clusters. Functional enrichment analysis highlighted key pathways, including Rap1 and MAPK kinases. Inhibitor experiments confirmed that the disruption of phosphorylation signaling impaired the integrity of the blood-testis barrier. Collectively, these findings demonstrated that androgens rapidly activate the protein phosphorylation signaling network in Sertoli cells, regulating critical processes such as blood-testis barrier formation, thereby providing new insights into male fertility and potential therapeutic strategies for spermatogenic disorders.

Correspondence to: Ms Ying Zhang or Mr. Qiong Deng, Department of Urology, Affiliated Longhua Hospital, Southern University of Science and Technology, 38 Jinglong Jianshe Road, Shenzhen, Guangdong 518109, P.R. China
E-mail: 21652766@qq.com
E-mail: dengqiong1987@smu.edu.cn

*Contributed equally

Abbreviations: AR, androgen receptor; EGFR, epidermal growth factor receptor; TMT, Tandem Mass Tag; HPLC-MS, high pressure liquid chromatography-mass spectrometry; DS, deviation score; SD, standard deviation; BTB, blood-testis barrier; ARE, androgen response elements; GO, Gene Ontology; KEGG, Kyoto Encyclopedia of Genes and Genomes

Key words: androgen, Sertoli cells, phosphorylation, blood-testis barrier, nonclassical pathways, caveolin-1

Introduction

Androgens are required for male fertility, mediating their effects primarily through genomic changes induced by androgen receptor (AR) and subsequent nuclear gene transcription. However, androgen also signals via rapid, non-classical pathways initiated at the cell membrane (1). Sertoli cells serve as notable mediators of androgen signals to germ cells. The AR signaling pathway regulates Sertoli cell proliferation and maturation and maintains the integrity of the blood-testis barrier (BTB) formed between adjacent Sertoli cells (2). Under AR signaling regulation, spermatogonial stem cells achieve a balance between self-renewal and differentiation. Furthermore, meiotic and post-meiotic processes, including Sertoli cell-spermatid attachment and spermatid development, are also AR-dependent, culminating in sperm release (2). Unlike the rapid non-classical effects observed within seconds (3), notable transcription changes are not detected until 30-45 min after hormonal stimulation (4). To date, three types of non-classical signaling pathway have been identified in the testis (5,6).

In the classical pathway, upon elevation of circulating androgens, the steroid hormone diffuses across the cell membrane into the cytoplasm, binds to the AR, and then translocates to the nucleus. Subsequently, it binds to androgen response elements (AREs) within the chromatin, thereby inducing transcriptional activation or repression (7). Non-classical actions of androgen in Sertoli cells were initially identified as rapid (within seconds) increases in Ca^{2+} influx and plasma membrane depolarization, resulting from androgen-mediated changes in ion channel activity (8-10). Subsequent studies using cultured primary rat Sertoli cells revealed that androgen stimulation induced rapid and sustained increases in protein phosphorylation and activation, such as cAMP response element-binding protein (CREB), extracellular signal-regulated kinase (ERK) (11). In the TM4 Sertoli cell line, caveolin-1 facilitates the transport of cytoplasmic AR to the membrane (11,12). Upon binding to membrane-associated AR, testosterone interacts with Src kinase, which then phosphorylates the epidermal growth factor receptor (EGFR), activates Ras and ultimately initiates the MAPK cascade (Ras-Raf-MEK-ERK) (5,13). Additionally, phosphorylated Akt can also activate Src, thereby further promoting the translocation of cytoplasmic AR to the plasma membrane (3).

To comprehensively elucidate the phosphorylation signaling pathways induced by androgens in Sertoli cells, tandem mass tag (TMT)-based high-depth phosphoproteomics was employed to establish a global protein phosphorylation profile. The role of these signaling pathways in the spermatogenesis and male fertility were further investigated. The present study aimed to provide a valuable resource offering novel insights into the non-classical actions of androgens, and to enrich the current understanding of androgen signaling and provide a theoretical foundation for the treatment of male infertility resulting from impaired spermatogenesis.

Materials and methods

Primary culture of mouse testicular Sertoli cells. The method was adapted from a previously published study (14). All animal procedures were approved by the Institutional Animal Care and Use Committee of the People's Hospital of Longhua, Shenzhen (also known as Affiliated Longhua Hospital, Southern University of Science and Technology; Shenzhen, China; approval no. LHRY-2106001; date of approval June 3, 2021), and all efforts were made to minimize animal suffering. Briefly, 21-day-old male C57BL/6J mice, purchased from the Guangdong Province Experimental Animal Center and were euthanized by cervical dislocation. The testes were harvested, washed three times with PBS, and the tunica albuginea was removed. The testicular tissue was placed in 0.5 mg/ml collagenase (Sigma) supplemented with 2% FBS (Gibco) and digested at 37˚C for 10 min. An equal volume of PBS was added, and the tissue was allowed to settle. This washing step was repeated 3-4 times until the supernatant became clear. The suspension was then centrifuged at 100 x g for 2 min at room temperature. Subsequently, 500 μl of DMEM/F12 medium (Gibco; Thermo Fisher Scientific, Inc.) was added, and the testicular tissue was minced. After mincing, 1 mg/ml trypsin (Sigma), 0.4 mg/ml DNase (Sigma) and 0.5 mg/ml hyaluronidase (Sigma) were added. The tissue was gently pipetted and digested at 37˚C for 15 min. A trypsin inhibitor (MillporeSigma) was then added to stop the digestion, and the cell suspension was filtered through a 100 μm cell strainer (Falcon; Corning Life Sciences). Cells were collected by centrifugation at 60 x g for 5 min at room temperature, washed once with DMEM/F12 medium, resuspended in complete culture medium and transferred to a cell culture incubator (37˚C, 5% CO_2). The complete medium consisted of DMEM/F12 supplemented with EGF (2.5 ng/ml, Thermo Fisher Scientific, Inc.), insulin (5 μg/ml; MilliporeSigma), transferrin (5 μg/ml; MilliporeSigma) and selenium (5 ng/ml; MilliporeSigma), gentamicin (50 μg/ml; MilliporeSigma) and bacitracin (5 μg/ml; MilliporeSigma). Cells plated in 6-cm culture dishes and allowed to reach 80-85% confluence were shifted to serum-free medium supplemented with 0.1% BSA. Following a 6-hour incubation period, the cells were exposed to 10 nM testosterone (3,12) (MeilunBio) for 5, 10 15, 30 and 60 min in a cell culture incubator (37˚C, 5% CO_2). Testosterone was dissolved in absolute ethanol to prepare a 10 mM stock solution. At the end of each treatment period, the medium was rapidly removed, and the cells were washed twice with ice-cold PBS. The cells were then processed according to the downstream assay. Sertoli cell purity was determined by immunostaining for SOX9 and DAPI nuclear counterstaining. The percentage of SRY-box transcription factor 9 (SOX9)-positive nuclei among total DAPI-positive nuclei was calculated from >500 cells per biological replicate across five random fields.

Cell immunofluorescence. Primary Sertoli cells were seeded onto glass coverslips at a density of $1x10^5$ cells/ml. For the protein phosphorylation inhibition study, cells were pre-incubated with 10 nM or 100 nM staurosporine for 2 h in a cell culture incubator (37˚C, 5% CO_2) (MedChemExpress). The concentration of 10 nM was selected because it falls within the established IC50 range for relatively selective protein kinase C (PKC) inhibition (IC50: 6-10 nM) (15). The concentration of 100 nM was selected to achieve broad-spectrum kinase inhibition, as previously used in rat Sertoli cell studies (16). The culture medium was then discarded, and cells were washed twice with PBS and fixed with 4% paraformaldehyde for 10 min at room temperature. After one PBS wash, cells were permeabilized with 0.1% Triton X-100 for 10 min at room temperature. Following two additional PBS washes, cells were blocked with 5% BSA (Solarbio) at room temperature for 30 min. Cells were then incubated overnight at 4˚C with rabbit IgG (negative control) or rabbit primary antibody against zonula occludens-1 (ZO-1) (1:200; 33-9100; Invitrogen) or SOX-9 (1:200; AB5535; Millipore). After three washes with PBS, the cells were incubated with a fluorescent secondary antibody (goat anti-rabbit IgG; 1:500; cat. no. A-11008; Invitrogen; Thermo Fisher Scientific, Inc.) at 37˚C for 1 h. DAPI was then added for an additional 5 min incubation at 37˚C. Finally, cells were washed three times with PBS, mounted with anti-fade mounting medium, and imaged using a laser scanning confocal microscope.

Protein phosphorylation mass spectrometry (MS) analysis. Cell pellets were resuspended in lysis buffer (PTM BIO LLC) containing 1% protease inhibitor cocktail and 1% phosphatase inhibitor cocktail. The samples were then sonicated on ice at a frequency of 20 kHz, with an amplitude of 30%. Sonication was performed in three 10 sec pulses (10 sec on, 10 sec off) to prevent heating. After sonication, lysates were centrifuged at 12,000 x g for 15 min at 4˚C, and the supernatants were collected as total cell lysates. Proteins concentration was determined using the BCA assay (Beyotime Biotechnology). Protein samples were digested overnight with trypsin (1:50; m: m; Promega Corporation) at 37˚C. Subsequently, dithiothreitol was added, and samples were reduced at 56˚C for 30 min. Iodoacetamide was then added, and the mixture was incubated at room temperature in the dark for 15 min. The resulting peptides were labeled using a TMT reagent kit (cat. no. 90068; Thermo Fisher Scientific, Inc.) according to the manufacturer's instructions. Labeled peptides were fractionated by high-pH reverse-phase high-performance liquid chromatography (HPLC). The fractions were dissolved in enrichment buffer (50% acetonitrile/6% trifluoroacetic acid) and gently incubated on a rotary shaker. After washing the resin three times, modified peptides were eluted with ammonia water. The eluate was collected, concentrated to dryness in a vacuum centrifuged, desalted and dried again. Peptides were then separated via an ultra-HPLC system (EASY-nLC 1200, Thermo Fisher Scientific, Inc.), ionized via an NSI ion source in positive

ion mode, and analyzed using a Q Exactive™ HF-X mass spectrometer (Thermo Fisher Scientific, Inc.).

Data analysis. The raw files generated from mass spectrometry were processed. A sample-specific protein database was constructed based on the sample origin, and database searching was performed using specialized analysis software. Quality control analysis was conducted at both the peptide and modification site levels based on the search results. To analyze temporal phosphorylation dynamics, the Mfuzz method (17) was employed to perform expression pattern clustering analysis on protein modification levels across consecutive time points following testosterone treatment. This method utilizes the fuzzy c-means clustering algorithm, which reduces the interference of noise on clustering results and effectively defines the relationship between genes/proteins and clusters. To further characterize the biological processes associated with proteins within each cluster, enrichment analyses for gene ontology (GO) functions (https://www.geneontology.org/), Kyoto Encyclopedia of Genes and Genomes (KEGG) pathways (https://www.genome.jp/kegg/) and protein domains were performed separately for the proteins in each cluster.

Results

Protein phosphorylation profiling. Androgen induces rapid protein kinase phosphorylation in Sertoli cells, and AR trafficking is mediated by the phosphorylation pathways (3). Previous phosphorylation signaling antibody array data and western blots revealed that several phosphorylation sites, including MEK1/2 (Ser217/221), AKT (Ser473), and ERK1/2 (Thr202/Tyr204), were rapidly phosphorylated within 5 min of stimulation; phosphorylation levels subsequently decrease and returned to basal levels by 15 min (3).

To comprehensively identify the phosphorylation signaling pathways activated by androgens, we applied HPLC-MS to screen for differentially modified kinases in mouse Sertoli cells. Sertoli cells were cultured in Serum-free medium for 6 h and then treated with 10 nM testosterone (3,12) for 5, 10 15, 30 and 60 min (Fig. 1A). Immunostaining with an antibody against SOX-9 confirmed that Sertoli cell purity >95% (Fig. 1B). Proteins were extracted and submitted to PTM BIO LLC for HPLC-MS analysis.

For protein identification, a total of 198,593 spectra were obtained, revealing 16,622 phosphorylation sites, of which 13,015 were quantifiable, corresponding with 4,154 quantifiable proteins (Fig. 1C). The motif characteristics of the modification sites were analyzed using the MoMo analysis tool based on the motif-x algorithm. All identified modification sites, along with 6 upstream and downstream amino acids for each, constituted the peptide sequences used for analysis. A characteristic peptide sequence was considered a motif if the number of peptides containing that sequence exceeded 20 peptides and the statistical P<0.000001. Based on the iceLogo analysis results, a heatmap (Fig. 1D) was used to display the degree of change in the frequency of amino acids flanking the modification sites, represented by the deviation score (DS). The DS was calculated using the formula: $DS=-Log_{10}(P\text{-value}) \times$ sign function (difference percent). Upstream and downstream amino acid D, E, P and S showed increased frequency.

Cluster analysis of differentially modified proteins. To characterize temporal changes in protein phosphorylation following testosterone treatment, the Mfuzz method was applied to perform cluster analysis across different time points. A total of 16,622 proteins were identified through quantitative proteomics analysis (Fig. 1B). To screen for proteins with significantly altered phosphorylation levels across the control, 5, 10, 15, 30 and 60 min time points, the relative modification levels of proteins were first log2-transformed, and proteins with a standard deviation (SD) >0.3 were selected. This cut-off was chosen based on the empirical distribution of the dataset, an SD threshold of 0.3 captured ~75% of the most variable phosphorylation sites while excluding sites with low technical noise. After filtering, 330 proteins were retained for pattern clustering analysis using the Mfuzz method. The parameters for Mfuzz analysis were set as follows: The number of clusters (k) was set to 6, and the fuzziness parameter (m) was set to 2. The Mfuzz expression pattern clustering diagram is shown in Fig. 2, the 330 proteins were clustered into 6 distinct clusters. In this analysis, line charts were generated to represent protein expression patterns, accompanied by corresponding heatmaps for each of the six identified clusters. For the line charts, the x-axis indicated the sample time points, while the y-axis represented the relative expression levels of the proteins. Each individual line within a chart corresponded to a single protein, and its color denoted the membership degree of that protein within its assigned cluster. In the associated heatmaps, the x-axis again represented the sample time points, and the y-axis listed the individual proteins. The color intensity in each heatmap reflected the relative expression level of each protein across the time-course samples. The proteins and the modified sites in different clusters were provided in Table SI.

Functional enrichment analysis. To investigate the biological characteristics of proteins within each cluster, enrichment analysis was performed for three categories: GO, KEGG pathways and protein domains. Fisher's exact test was employed, and terms with a P<0.05 were considered significantly enriched. As shown in the KEGG pathway enrichment clustering heatmap, cluster 6 were predominantly enriched in signaling pathways, including the 'Rap1 signaling pathway', which regulates cell junctions and adhesion (18) (Fig. 3A). The GO biological process enrichment clustering heatmap (Fig. 3B) revealed that cluster 5 and cluster 6 are mainly enriched in 'activation of GTPase activity' (cluster 5) (19), 'centrosome localization' and 'positive regulation of DNA synthetic process' (cluster 6). Regarding GO molecular function both clusters were enriched in terms related to 'protein kinase activity', and cluster 6 was also enriched in 'MAP kinase kinase activity' (Fig. 3C). The protein domain enrichment clustering analysis showed that cluster 6 were enriched in 'protein kinase domains' (Fig. 3D). Finally, GO cellular component enrichment clustering revealed that cluster 6 includes 'caveola' (Fig. 3E). This finding is consistent with our previous report that caveolin-1 on the cell membrane interacts with AR, mediating the rapid non-classical pathways of androgen action (12). Full lists of significantly enriched GO terms, KEGG pathways and protein domains, along with their corresponding P-values, are provided in Table SII.

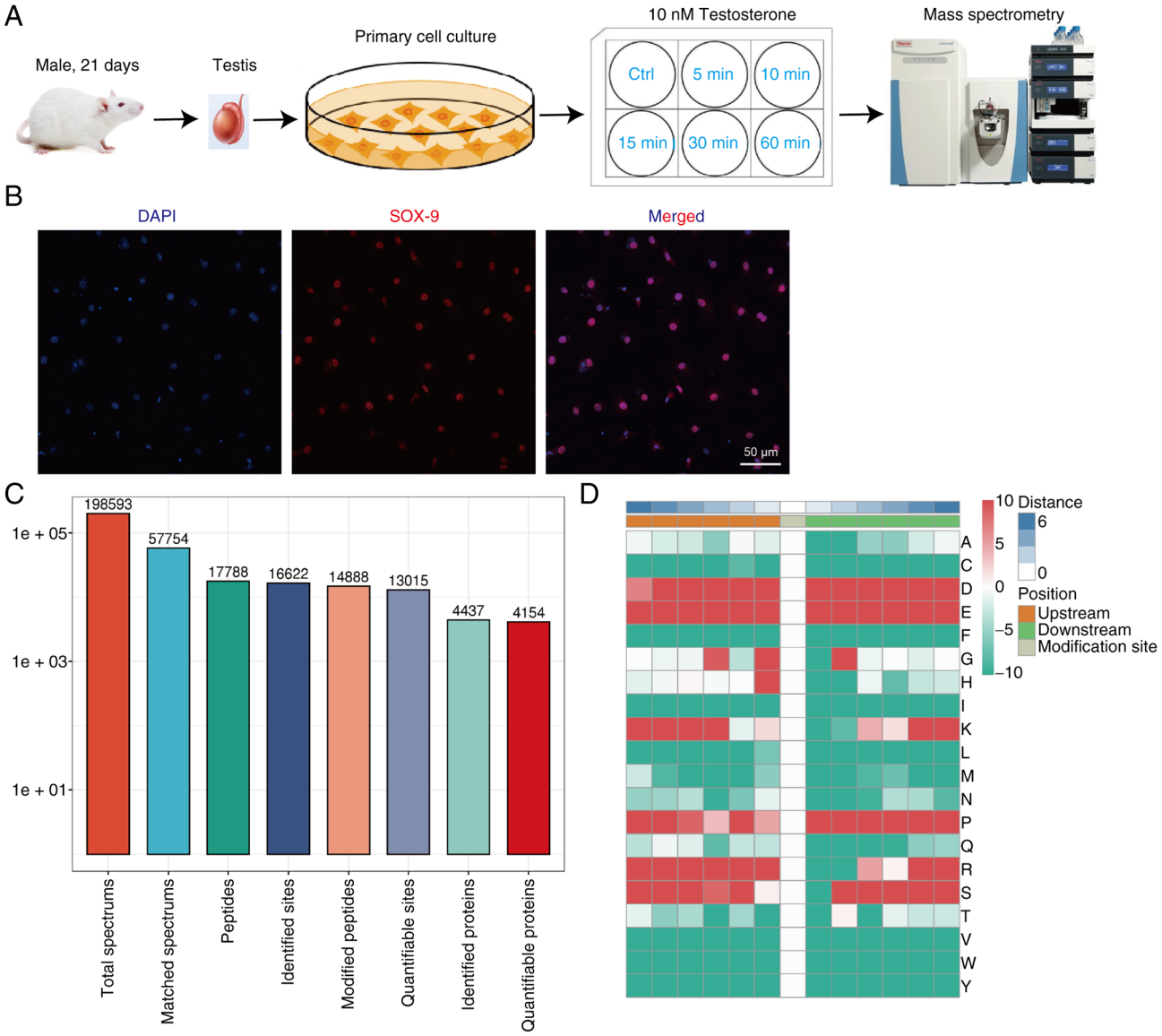

Figure 1. Protein phosphorylation profiling. (A) A flow chart of the study is presented. (B) *Sertoli* cell identity was confirmed by SOX-9 immunostaining. Red fluorescence, SOX-9; blue, DAPI. (C) The overview of label-free quantification-based quantitative protein phosphorylation identification is shown. (D) The motif characteristics of the modification sites are displayed.

Blockade of phosphorylation signaling pathways disrupts BTB integrity. Primary Sertoli cells were isolated from 21-day-old mice and treated with staurosporine, a broad-spectrum protein phosphorylation inhibitor. The integrity of the BTB was assessed by evaluating the continuous localization of ZO-1, a BTB-associated marker protein, at the interfaces between adjacent *Sertoli* cells (Fig. 4). Compared with the control group, the 10 nM staurosporine treatment group exhibited compromised BTB formation between adjacent Sertoli cells. In the 100 nM treatment group, BTB formation was almost completely absent, as indicated by the loss of continuous linear ZO-1 staining at intercellular junctions, which appeared fragmented or discontinuous instead. These findings demonstrate that inhibition of phosphorylation signaling pathways impairs BTB integrity in primary Sertoli cells. Collectively, these results suggest that the AR regulates BTB formation through rapid phosphorylation signaling pathways, thereby playing a notable role in the process of spermatogenesis.

Discussion

Over the years, male semen quality has been progressively declined, and the number of men experiencing infertility has increased annually (20,21). Consequently, male reproductive health has garnered growing attention. Impaired spermatogenesis is a major cause of male infertility (22). The World Health Organization ranks infertility as the third most significant disease after cancer and cardiovascular diseases (23). Therefore, elucidating the molecular mechanisms underlying spermatogenic disorders and identifying effective treatments for male infertility are priorities in reproductive medicine research.

Studies have indicated that the non-classical pathway of androgen-AR is necessary for germ cell-*Sertoli* cell adhesion during spermatogenesis, whereas the classical pathway is not (5,24,25). Testosterone concentrations in testicular tissue exceed the levels required for transcriptional regulation via

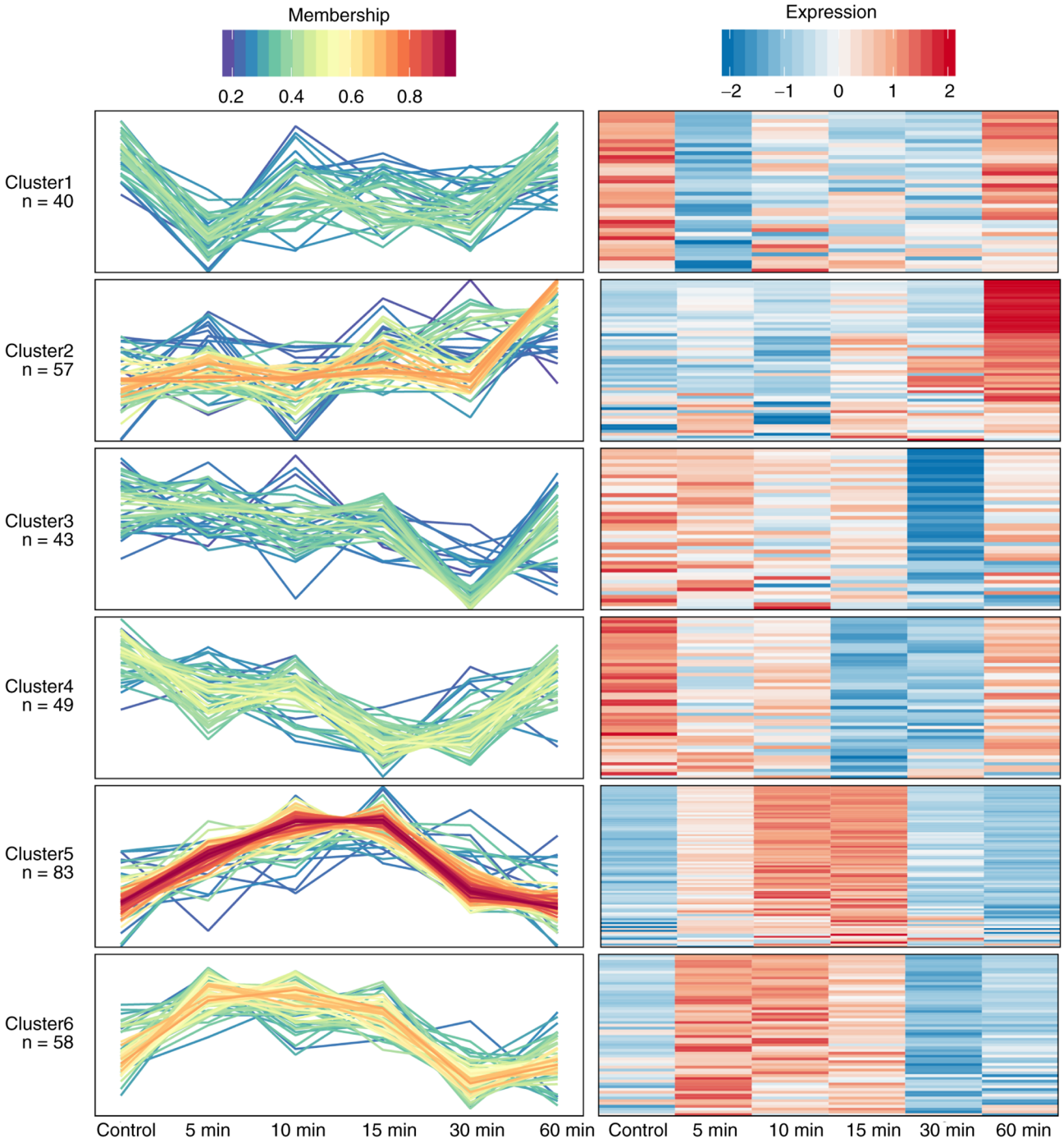

Figure 2. Mfuzz expression pattern clustering diagram. The left panel shows line charts of protein expression levels, while the right panel displays heatmaps of expression levels. Each cluster corresponds to one line chart and one heatmap. For the line chart, the x-axis represents the samples, and the y-axis represents the relative expression levels of proteins. Each line corresponds to an individual protein, and the line color indicates the membership degree of the protein in the current cluster. For the heatmaps, the x-axis represents the samples and the y-axis represents different proteins. The color intensity in the heatmap reflects the relative expression level of each protein in the samples.

androgen response elements (ARE). Moreover, researchers have identified only a limited number of androgen-regulated genes in Sertoli cells, with only a subset being regulated through ARE. Consequently, research focus has shifted toward the rapidly activated kinase signaling pathways induced by androgens (26,27). These signaling pathways can alter gene expression independently of ARE or AR promoter activity and are characterized by rapid onset and robust effects.

Androgens rapidly activate protein kinase phosphorylation in *Sertoli* cells via AR (3), a temporal expression pattern resembling that of clusters 5 and 6 shown in the present study. In the present study, phosphoproteomics technology was employed to systematically map the dynamic landscape of phosphorylation signaling in mouse testicular Sertoli cells following androgen stimulation. A total of 13,015 quantifiable phosphorylation sites were successfully identified, and through time-series clustering analysis, revealed

Figure 3. Functional enrichment analysis. (A) The Kyoto Encyclopedia of Genes and Genomes pathway enrichment cluster heatmap is illustrated. (B) This panel shows GO biological process functional enrichment cluster heatmap. (C) Panel C displays the GO molecular function functional enrichment cluster heatmap. (D) Depicted here is the protein domain enrichment cluster heatmap. (E) The GO cellular component functional enrichment cluster heatmap is provided. GO, gene ontology. The color scale represents the fold change (log2 scale), not P-values.

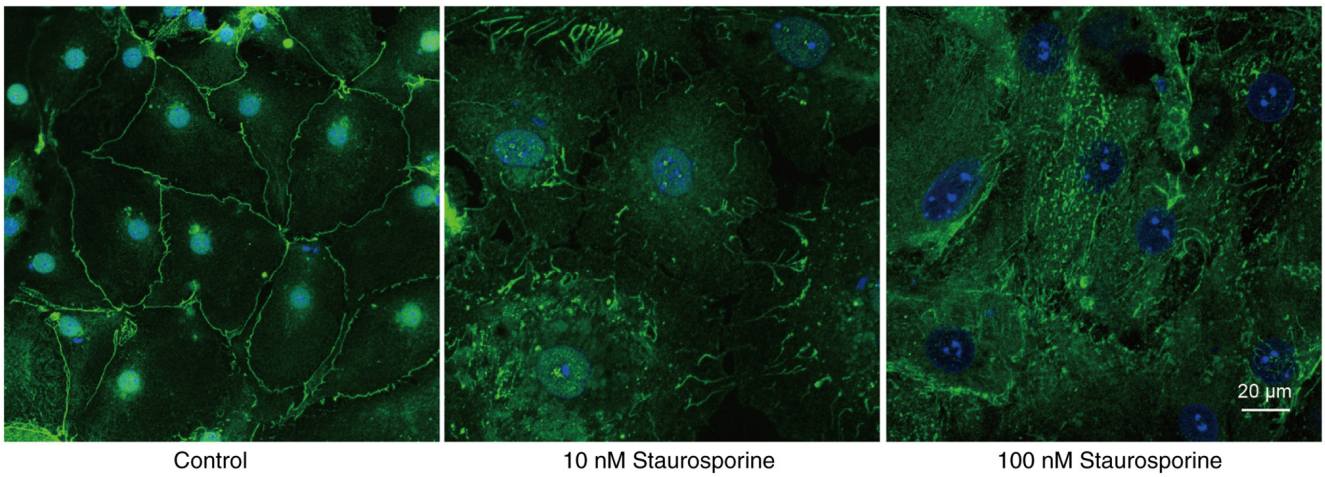

Figure 4. Effect of the protein phosphorylation inhibitor staurosporine on blood-testis barrier formation in mouse testicular Sertoli cells. Green fluorescence, ZO-1; blue, DAPI.

that androgen-activated signaling pathways exhibit rapid, transient and diverse characteristics. Notably, the rapid phosphorylation and subsequent attenuation pattern observed for proteins in clusters 5 and 6 aligns with the activation kinetics of key kinases such as MEK/ERK and Akt, as previously reported (3). Results from phosphorylation signaling pathway antibody arrays and western blot analysis demonstrated that testosterone induces rapid phosphorylation at multiple sites, including MEK1/2 (Ser217/221), AKT (Ser473) and ERK1/2 (Thr202/Tyr204), within 5 min, after which kinase phosphorylation levels gradually decline and return to baseline (3). Functional enrichment analysis further confirmed that these rapid androgen-regulated proteins are notably enriched in signaling pathways such as Rap1 and MAPK kinases, as well as in crucial biological processes including cell junction and adhesion and cell division. These findings provide support at the omics level for the hypothesis that the androgen-AR non-classical pathway regulates cellular functions through a rapid phosphorylation network.

Notably, at the cellular component level, it was found that cluster 6 is notably associated with the caveola structure. This discovery aligns with our previous research (12), together constructing a clearer molecular picture; caveolae structures formed by Caveolin-1 on the cell membrane likely serves as core platforms for initiating non-classical pathway signaling by androgens. These platforms mediate the membrane translocation of AR and efficiently assemble and activate downstream Src/EGFR/MAPK cascades there. In addition to clusters 5 and 6, which exhibited the most pronounced testosterone-induced phosphorylation changes; however, clusters 1-4 also displayed distinct temporal dynamics. Cluster 2 maintained stable baseline phosphorylation levels until 30 min, followed by a rapid increase at 60 min. Clusters 1, 3 and 4 shared a common pattern, characterized by a decrease between 5 and 30 min, then a rapid phosphorylation peak at 60 min. Although these clusters were not the primary focus of the present study, they exhibited distinct temporal dynamics and were not further investigated here due to the scope of this work. Nevertheless, they represent valuable candidates for future hypothesis-driven research on delayed androgen signaling and may point to additional regulatory mechanisms warranting future investigation.

To preliminarily validate the functional significance of these phosphorylation events, cells were treated with the broad-spectrum kinase inhibitor staurosporine. Consistent with the rapid phosphorylation patterns observed in clusters 5 and 6, the present experimental results showed that inhibiting overall phosphorylation signaling markedly disrupts BTB integrity. Specifically, staurosporine treatment notably abolished testosterone-induced phosphorylation changes, directly demonstrating that rapid phosphorylation signaling pathways are essential for androgens to maintain BTB function in Sertoli cell. Given that staurosporine is a broad-spectrum kinase (28) inhibitor, these findings suggest that the phosphorylation events within clusters 5 and 6 are mediated by staurosporine-sensitive kinases, which could potentially include PKC and other serine/threonine kinases. Further studies using selective inhibitors will be required to delineate the specific contribution of individual kinases. Androgens likely maintain BTB integrity and Sertoli cell-germ cell adhesion by rapidly activating signaling pathways such as Rap1 and MAPK, thereby regulating the phosphorylation of substrates, including cell junction proteins.

A potential mechanistic model linking caveolae, AR trafficking, Src/EGFR/MAPK signaling and BTB proteins such as ZO-1 can be proposed based on the present phosphoproteomic data and existing literature. Caveolae, cholesterol-rich membrane invaginations, have been implicated in AR membrane trafficking and signaling complex assembly (12). Upon testosterone stimulation, caveolae may facilitate AR translocation to the membrane, where it interacts with Src kinase, leading to Src activation. Activated Src then transactivates EGFR, triggering the downstream MAPK (ERK1/2) cascade (5). This signaling axis ultimately converges on BTB-associated proteins, including ZO-1, where phosphorylation events may regulate tight junction dynamics and barrier permeability; however, direct evidence was not performed in the present study. Nevertheless, the present findings provide

a phosphoproteomic resource that supports this integrated model and generates testable hypotheses for future mechanistic studies.

Several limitations of the present study should be acknowledged. First, all experiments were conducted exclusively using the primary mouse Sertoli cell line, which may not fully recapitulate the complexity of *in vivo* physiology micro-environment or human physiology. Second, the present findings are derived from *in vitro* experiments; *in vivo* verification using animal models will be essential to confirm the biological relevance of the observed phosphorylation changes. Third, staurosporine was used as a broad-spectrum kinase inhibitor, while effective in blocking phosphorylation events, it may have off-target effects on non-androgen pathways. Therefore, the present conclusions regarding specific signaling pathways are preliminary, and follow-up studies using selective inhibitors are needed. Future studies employing primary Sertoli cells, *in vivo* models and targeted kinase perturbations are warranted to validate and extend the present conclusions.

In summary, the novelty lies in using time-resolved phosphoproteomics to reveal that testosterone rapidly activates caveolae-associated and MAPK/Rap1 phosphorylation networks in primary Sertoli cells, which are essential for blood-testis barrier integrity. The present study provides a comprehensive resource for understanding the rapid non-classical signaling networks activated by androgens in testicular *Sertoli* cells. The present findings reveal that: i) Testosterone induces time-dependent phosphorylation changes clustering into six distinct temporal patterns; ii) clusters 5 and 6 are most responsive, enriched in caveolae-associated and Src/EGFR/MAPK signaling pathways; and iii) BTB proteins including ZO-1 are potential downstream targets of this signaling axis. The key phosphorylation signaling nodes revealed in the present study-such as specific kinases within the Rap1 and MAPK pathways, hold promise as important candidates for future development of diagnostic biomarkers or therapeutic targets for male infertility. Collectively, these insights offer novel perspectives and potential therapeutic strategies for addressing male infertility caused by impaired spermatogenesis.

Acknowledgements

Not applicable.

Funding

The present study was supported by grants from Shenzhen Science and Technology Program (grant nos. JCYJ202408 13114409013 and JCYJ20230807145102005) and Medical Research Special Project of Shenzhen Longhua Medical Association (grant no. 2023LHMA08).

Availability of data and materials

The raw mass spectrometry proteomics data generated in the present may be found in iProX under the accession number IPX0017310000 or at the following URL: https://www.iprox.cn/page/subproject.html?id=IPX0017310002. All other data generated or analyzed during the present study may be requested for the corresponding author.

Authors' contributions

QD, YZ and HL conceptualized the study and designed the experiments and data analysis methods. RS, YD, LG and ZW conducted all experiments and performed the data analysis. QD, YZ and ZW prepared the figures, analyzed the data and drafted the manuscript. QD and YZ confirm the authenticity of all the raw data. All authors have read and approved the final version of the manuscript and agree to be accountable for all aspects of the work.

Ethics approval and consent to participate

All the mice were treated according to the Guide for the Care and Use of Laboratory Animals prepared by the Institute of Laboratory Animal Resources for the National Research Council. The study was approved by the ethics committee of the People's Hospital of Longhua, Shenzhen (also known as Affiliated Longhua Hospital, Southern University of Science and Technology; approval no. LHRY-2106001; date of approval: June 3, 2021). All efforts were made to minimize animal suffering throughout the experiments.

Patient consent for publication

Not applicable.

Competing interests

The authors declare that they have no competing interests.

References

1. Cooke PS and Walker WH: Nonclassical androgen and estrogen signaling is essential for normal spermatogenesis. Semin Cell Dev Biol 121: 71-81, 2022.
2. Wang JM, Li ZF and Yang WX: What does androgen receptor signaling pathway in sertoli cells during normal spermatogenesis tell us? Front Endocrinol (Lausanne) 13: 838858, 2022.
3. Deng Q, Zhang Z, Wu Y, Yu WY, Zhang J, Jiang ZM, Zhang Y, Liang H and Gui YT: Non-genomic action of androgens is mediated by rapid phosphorylation and regulation of androgen receptor trafficking. Cell Physiol Biochem 43: 223-236, 2017.
4. Shang Y, Myers M and Brown M: Formation of the androgen receptor transcription complex. Mol Cell 9: 601-610, 2002.
5. Walker WH: Non-classical actions of testosterone and spermatogenesis. Philos Trans R Soc Lond B Biol Sci 365: 1557-1569, 2010.
6. Kabbesh H, Bulldan A, Konrad L and Scheiner-Bobis G: The role of ZIP9 and androgen receptor in the establishment of tight junctions between adult rat sertoli cells. Biology (Basel) 11: 668, 2022.
7. Tsai MJ and O'Malley BW: Molecular mechanisms of action of steroid/thyroid receptor superfamily members. Annu Rev Biochem 63: 451-486, 1994.
8. Lyng FM, Jones GR and Rommerts FF: Rapid androgen actions on calcium signaling in rat sertoli cells and two human prostatic cell lines: Similar biphasic responses between 1 picomolar and 100 nanomolar concentrations. Biol Reprod 63: 736-747, 2000.
9. Von Ledebur EI, Almeida JP, Loss ES and Wassermann GF: Rapid effect of testosterone on rat sertoli cell membrane potential. Relationship with K+ATP channels. Horm Metab Res 34: 550-555, 2002.

10. Loss ES, Jacobsen M, Costa ZS, Jacobus AP, Borelli F and Wassermann GF: Testosterone modulates K(+)ATP channels in sertoli cell membrane via the PLC-PIP2 pathway. Horm Metab Res 36: 519-525, 2004.
11. Fix C, Jordan C, Cano P and Walker WH: Testosterone activates mitogen-activated protein kinase and the cAMP response element binding protein transcription factor in Sertoli cells. Proc Natl Acad Sci USA 101: 10919-10924, 2004.
12. Deng Q, Wu Y, Zhang Z, Wang Y, Li M, Liang H and Gui Y: Androgen receptor localizes to plasma membrane by binding to caveolin-1 in mouse sertoli cells. Int J Endocrinol 2017: 3985916, 2017.
13. Begley MJ, Yun CH, Gewinner CA, Asara JM, Johnson JL, Coyle AJ, Eck MJ, Apostolou I and Cantley LC: EGF receptor specificity for phosphotyrosine-primed substrates provides signal integration with Src. Nat Struct Mol Biol 22: 983-990, 2015.
14. Tang EI and Cheng CY: MARK2 and MARK4 regulate sertoli cell BTB dynamics through microtubule and actin cytoskeletons. Endocrinology 163: bqac130, 2022.
15. Kageyama M, Mori T, Yanagisawa T and Taira N: Is staurosporine a specific inhibitor of protein kinase C in intact porcine coronary arteries? J Pharmacol Exp Ther 259: 1019-1026, 1991.
16. Lambert A, Talbot JA, Mitchell R and Robertson WR: Inhibition of protein kinase C by staurosporine increases estrogen secretion by rat sertoli cells. Acta Endocrinol (Copenh) 125: 286-290, 1991.
17. Futschik ME and Carlisle B: Noise-robust soft clustering of gene expression time-course data. J Bioinform Comput Biol 3: 965-988, 2005.
18. Xiaoxia F, Rui L, Meiru C, Lu Y and Ying J: CD147 regulates the Rap1 signaling pathway to promote proliferation, migration, and invasion, and inhibit apoptosis in colorectal cancer cells. Sci Rep 15: 20237, 2025.
19. Pan ZN, Zhang HL, Zhang KH, Ju JQ, Liu JC and Sun SC: Insufficient MIRO1 contributes to declined oocyte quality during reproductive aging. Sci China Life Sci 68: 764-776, 2025.
20. Virtanen HE, Jørgensen N and Toppari J: Semen quality in the 21st century. Nat Rev Urol 14: 120-130, 2017.
21. Chen J, Guo JM, Jiang BJ, Sun FY and Qu YC: Impact of physical activity on semen quality: A review of current evidence. Asian J Androl 27: 574-580, 2025.
22. Bhattacharya I, Sharma SS and Majumdar SS: Etiology of male infertility: An update. Reprod Sci 31: 942-965, 2024.
23. Esteves SC: The WHO 2025 guideline for the prevention, diagnosis and treatment of infertility: A comprehensive review with focus on male reproductive health. Int Braz J Urol 52: e20260121, 2026.
24. Toocheck C, Clister T, Shupe J, Crum C, Ravindranathan P, Lee TK, Ahn JM, Raj GV, Sukhwani M, Orwig KE and Walker WH: Mouse spermatogenesis requires classical and nonclassical testosterone signaling. Biol Reprod 94: 11, 2016.
25. Shupe J, Cheng J, Puri P, Kostereva N and Walker WH: Regulation of sertoli-germ cell adhesion and sperm release by FSH and nonclassical testosterone signaling. Mol Endocrinol 25: 238-252, 2011.
26. Walker WH: Nongenomic actions of androgen in sertoli cells. Curr Top Dev Biol 56: 25-53, 2003.
27. Rahman F and Christian HC: Non-classical actions of testosterone: An update. Trends Endocrinol Metab 18: 371-378, 2007.
28. Davis MI, Hunt JP, Herrgard S, Ciceri P, Wodicka LM, Pallares G, Hocker M, Treiber DK and Zarrinkar PP: Comprehensive analysis of kinase inhibitor selectivity. Nat Biotechnol 29: 1046-1051, 2011.